13th ewtec 2019 Proceedings of the 13th European Wave and Tidal Energy Conference 1-6 Sept 2019, Naples, Italy

Analytical and physical modelling of a quayside Wave Energy Converter (WEC) and study of its impact on overtopping

Sixtine Neuvéglise, Gaële Perret, Hassan Smaoui, François Marin and Philippe Sergent

Abstract—**This paper considers the behaviour of a Wave Energy Converter (WEC) placed in front of a vertical sea wall. The aim of this work is twofold: study the effect of the Power Take Off (PTO) on a WEC behaviour and quantify the impact of the system on overtopping. The WEC is composed of a rectangular floater in heave motion and of a linear damper representing the PTO. In order to study the WEC motion amplitude and the overtopping, experimental results are compared with a linear analytical model based on potential flow theory. Concerning the analytical model, the WEC motion equation is expressed using hydrodynamic coefficients where added mass, damping and excitation force are solved using the eigenfunction matching method. The analytical overtopping is calculated using the wave elevation above the sea wall. Comparing both models, several results are highlighted. In the presence of the PTO, the analytical model is in good accordance with the experimental model. Moreover, the maximum efficiency obtained using experimental results is superior to 30%. It is reminded that no optimization was performed on the system dimensions. Finally, it is shown that the presence of the WEC can reduce the wave overtopping. On the other hand, the presence of the PTO does not much affect the overtopping. Results also show that the major parameters influencing the overtopping are the wave length, the toe clearance and the WEC draft.**

Index Terms—**Analytical modelling, physical modelling, quayside WEC, wave energy**

I. Introduction

MANY technologies of Wave Energy Converters (WEC) have been developed (for a complete description of the systems see [1]–[3]). WEC can be classified according to their technologies [4] but also according to their distance to the shore as offshore, nearshore or quayside systems. In order to reduce construction and maintenance costs, nearshore and quayside systems have been developed [5]. In this context, the present study is focused on quayside point absorber system. The problem is simplified by considering a rectangular WEC, moving in a heave motion along a vertical wall breakwater. The Power Take Off (PTO) of the WEC is represented by a linear damper [6].

Study a WEC behaviour can be realized by using different models as experimental, numerical or analytical models. Let us focus on analytical models. A first linear model has been developed by Andersen and Wuzhou [7] using the Green function and eigenfunctions to calculate the motion equation parameters of a floating buoy. Some years later, simplified formulae have been proposed by Drimer, Agnon and Stiassnie [8] to calculate the added mass and the damping. Based on those results, Zheng, You and Shen [9] proposed a linear analytical model able to calculate the hydrodynamic coefficients of a floating buoy based on the eigenfunction matching method. Following Zheng, You and Shen [9], Zheng et al. [10] enhanced the model by adding a sidewall beside a rectangular floater. More recently, a cylindrical floater has been considered in a 3D configuration ([11], [12]). Mavrakos et. al. [13] also studied the hydrodynamic characteristics of an array of cylindrical floaters in front of a vertical dike. Penalba, Kelly and Ringwood [14] proposed an analytical model based on the Boundary Element Method (BEM). The model NEMOH solves a floater behaviour by calculating the hydrodynamic coefficients based on the Green function resolution and a BEM formulation [15]. Roessling and Ringwood [16] compared NEMOH to the similar model WAMIT (http://www.wamit.com). They show that similar values of the radiated coefficients are obtained with the two models in the case of a heaving cylinder.

Due to the presence of nearshore or quayside systems, the coastal environment may be affected. In particular, Zanuttigh and Angelelli [17] proposed to use WECs to reduce the incident waves. Moreover, Stratigaki [18] outlined that incident wave attenuation and wave power reduction are affected by a WEC farm

1399-WDD - The project is co-financed by Cerema, and the Normandy council and European Union through ERDF funds (NEPTUNE project). We also express our thanks to the LHN laboratory and the Roberval laboratory (FRE CNRS 2012, Universit de Technologie de Compigne) for providing us with the necessary computer resources to carry out this study. We finally thank Ifremer in Boulogne-sur-Mer for their help and advices concerning the linear dampers.

S. Neuvglise is at the Laboratoire de Recherche en Eco-innovation Industrielle et nergtique (LR2E) at cole Suprieure dIngnieurs en Gnie lectrique, Productique et Management Industriel (ECAM-EPMI), 13 Bvd de l'Hautil, 95092 Cergy-Pontoise Cedex, France (e-mail: s.neuveglise@ecam-epmi.com)

H. Smaoui is at the Cerema - Direction Technique Eau Mer et Fleuves (DTechEMF), 134 rue de Beauvais - CS 60039, 60280 Margny-Ls-Compigne, France and at the Laboratoire Roberval-LHN, FRE CNRS 2012, Sorbonne Universit, Universit Technologique de Compigne (UTC), CS 60319, 60203 Compigne, France (e-mail: Hassan.Smaoui@cerema.fr)

F. Marin is at the Laboratoire Ondes et Milieux Complexes (LOMC), UMR CNRS 6294, Le Havre Normandie University, 53 rue du Prony, 76600 Le Havre, France (e-mail: francois.marin@univ-lehavre.fr)

P. Sergent is at the Cerema - Direction Technique Eau Mer et Fleuves (DTechEMF), 134 rue de Beauvais - CS 60039, 60280 Margny-Ls-Compigne, France (e-mail: Philippe.Sergent@cerema.fr)

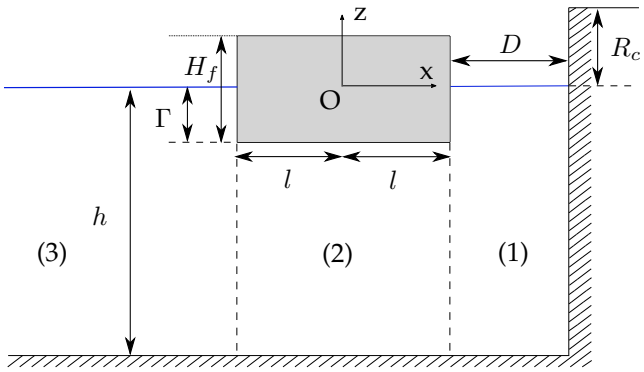

Fig. 1. Scheme of the system

positively of negatively. Mendoza et al. [19] studied the WEC behaviour acting as a coastal defence, using numerical simulations. Different methods can be used to estimate the overtopping. De Waal and Van Der Meer [20] proposed equations to calculate overtopping of different types of dike and breakwater. From these formulae, EurOtop 2016 [21] proposed safety design rules to avoid overtopping. In addition, Shao et al. [22] and Goda [23] proposed to use respectively numerical and experimental models to estimate overtopping.

This study has two main objectives. Firstly, the behaviour of the quayside point absorber and its efficiency are considered. Regular and irregular waves are used. Thereafter, the WEC impact on sea wall overtopping is analysed. Comparison between experimental and analytical models is used in order to understand the main parameters impacting the WEC behaviour and the overtopping.

First of all experimental and analytical models are described in sections 2 and 3, respectively. Section 4 is devoted to the study of the WEC behaviour and to its efficiency. The WEC impact on overtopping quantifications is presented in the following section 5. Finally conclusions and perspectives are given in section 6.

II. Experimental model

A. Device description

The studied system is composed of a rectangular WEC oscillating in heave motion, along a vertical wall breakwater. The system is represented in Fig. 1, where $2l$ is the floater width, Γ the draft, H_f the floater height and $H_f - \Gamma$ represents the air draft of the floater. The water depth is denoted h, the toe clearance D and R_c represents the crest free board of the sea wall. In order to consider a bidimensionnal configuration, the floater fills almost the whole width of the flume : a gap of 0.5 mm exists between each extremity of the floater and the flume walls. Two vertical spikes maintain the WEC near the sea wall and allow the system to move only in heave motion.

Experimental tests are performed at Le Havre Normandie University in a 34 m long, 0.90 m wide and 1.2 m high wave flume. A picture of the experimental device is given in Fig. 2. Active wave absorption is used for all tests in order to limit the standing waves in the flume. The incident and reflected waves amplitudes

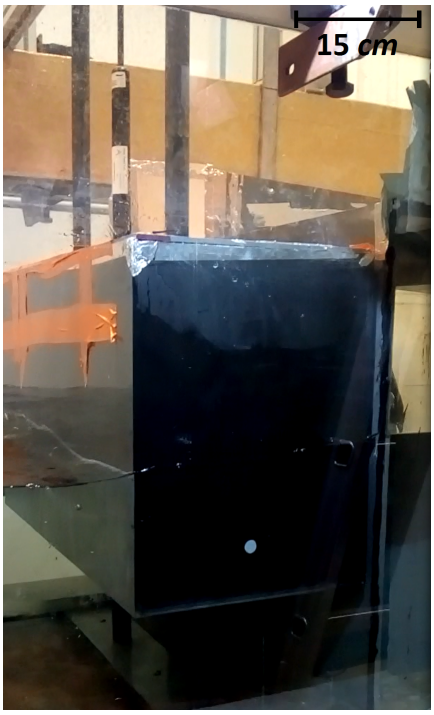

Fig. 2. Picture of one of the experimental device, with $\Gamma = 0.15$ m, $l = 0.15$ m, $H_f = 0.40$ m and $D = 0.01$ m

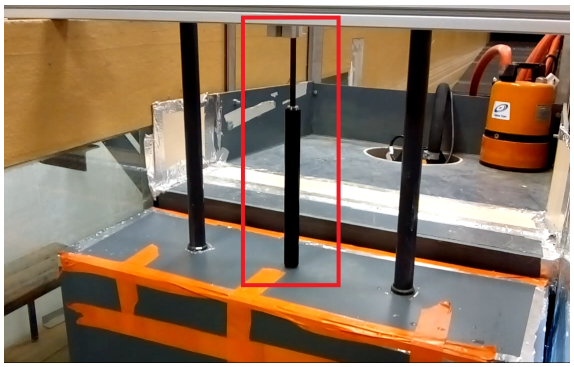

Fig. 3. Picture of the PTO fixed between the WEC and a fixed point

are calculated using the method developed by Mansard and Funke [24] and Goda and Suzuki [25] for regular and irregular waves, respectively, using four resistive probes. The closer probe is placed at 2.24 m from the WEC. The maximum uncertainty on wave amplitude measurement is about $\pm$ 1 mm. A CCD camera (Basler aca2040) tracks a target painted on the side of the WEC in order to measure its vertical position Z. Image analysis was performed using the MATLAB 'image processing' module. The maximum uncertainty on the WEC motion does not exceed 1 mm, leading to a maximum relative error of 3%.

The effects of the Power Take Off (PTO) on the WEC behaviour are represented by a linear adjustable damper. During a test, one extremity of the damper is fixed to the upper part of the WEC and the other extremity to a fixed point (Fig. 3). The damper has a maximum stroke of 250 mm and can deliver from 30 N to 3000 N. Two dampers HD 28/250 from Slam Proof Ltd are used, whose damping are adjusted at two different values. The damper with the lower damping is

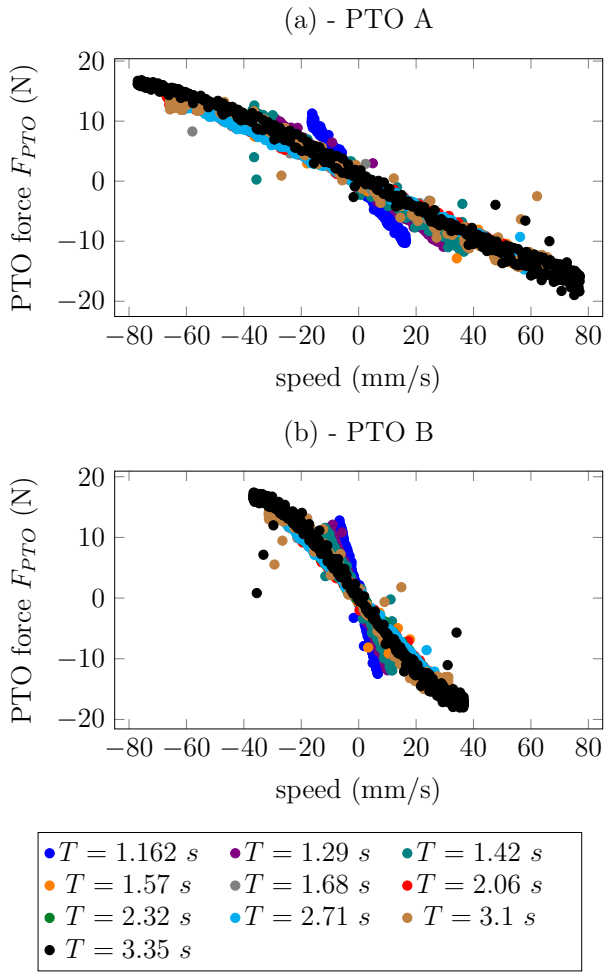

Fig. 4. Calibration curves for the two dampers for different wave periods (regular waves only)

called PTO A and the second with the higher damping is called PTO B. In order to characterize the dampers, a calibration is performed to obtain the relation between the displacement velocity and the damper force. The calibration table is composed of an electric damper (imposing a velocity thanks to the computer controls) and of a force sensor. In regular waves, sinusoidal velocities are imposed to the damper where the velocity amplitude corresponds to the mean measured velocity amplitude of the WEC at a given wave period T. Note that in irregular waves, the WEC velocity corresponds to the time derivative of the WEC position obtained by the camera during an experimental test.

The force values obtained at different periods T are plotted as a function of the damper velocity in Fig. 4 for regular waves. Two main results are observed. Firstly, the relation between the damping force and velocity is linear. Indeed, no hysteresis losses are observed in Fig. 4. Thus the relation between the damping force and the displacement velocity can be expressed following (1), where B_{PTO} is the slope of the calibration curves (representing the PTO coefficient) and $\dot{Z}$ is the displacement speed of the WEC in regular waves.

$$F_{PTO}(t) = B_{PTO}\dot{Z}(t) \quad (1)$$

Secondly, the slope B_{PTO} is increased for the smallest values of the wave period. Indeed, according to Fig. 5

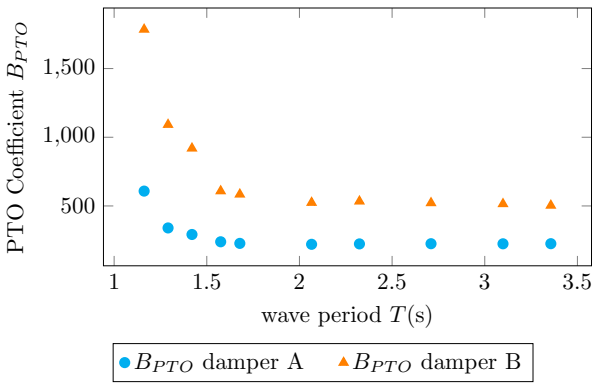

Fig. 5. Values of the B_{PTO} for PTO A and PTO B for all tested wave conditions (regular waves only)

where B_{PTO} is plotted as a function of the wave period, values of the B_{PTO} are constant for $T > 1.7$ s. For $T < 1.7$ s, values of the PTO coefficient B_{PTO} are strongly increased.

B. Experimental test conditions

Experimental tests are performed using regular and irregular wave conditions. In regular conditions, two WEC are tested whose dimensions and corresponding wave conditions are described in Table I. The floater 1 has the higher draft and is tested at one water depth. The floater 2 is larger than floater 1 but has a smaller draft. Tests realized with this floater are performed for different water depths. The incident wave height is equal to $H_i = 0.05$ m and the toe clearance is fixed at $D = 0.01$ m. Experimental tests are performed without PTO, with PTOA and PTOB successively for the two floaters.

	WEC dimensions			Regular wave conditions			
	l (m)	Γ (m)	D (m)	H_i (m)	ω (rad/s)	PTO	h (m)
1	0.05	0.25	0.01	0.05	5.41, 4.87, 4.42, 3.74, 3.04, 2.70, 2.03, 1.87	without, PTOA, PTOB	0.6
2	0.15	0.15	0.01	0.05	5.41, 4.42, 3.74, 3.24, 2.86, 2.56, 2.32	without, PTOA, PTOB	0.4, 0.5, 0.6

TABLE I
WEC DIMENSIONS AND REGULAR WAVE CONDITIONS.

The irregular waves are modelled using the Jonswap spectrum following (2) to (4), where $S(f)$ is the wave spectrum according to Hasselmann et al. [26], H_{m0} represents the significant wave height and ω_m the spectrum peak frequency. The coefficient γ is fixed at the value $\gamma = 3.3$ according to Michard et al. [27].

$$S(f) = \alpha \frac{f_p^4}{2\pi f^5} H_{m0}^2 \mathrm{e}^{\left(-\frac{5}{4}\left(\frac{f_p}{f}\right)^4\right)} \gamma^{\mathrm{e}^{\left(-\frac{1}{2}\left(\frac{(f-f_p)^2}{\sigma^2 f^2}\right)\right)}} \quad (2)$$

$$\text{with } \alpha \text{ defined with } m_o = \int S(f)df = \frac{H_{m0}^2}{16} \quad (3)$$

$$\text{and if } f < \frac{\omega_m}{2\pi},\ \sigma = 0.07 \quad \text{nor} \quad f > \frac{\omega_m}{2\pi},\ \sigma = 0.09 \quad (4)$$

The wave conditions used in irregular waves are inspired from an application site located in Esquibien in France according to Michard et al. [27] (see Table II). In irregular waves the floater 2 has been tested, located at a distance $D = 0.01$ m from the sea wall, at a water depth $h = 0.4$ m and with PTOA only.

		ω_m (rad/s)					
		5.40	4.42	3.74	3.25	2.86	2.56
H_{m0} (m)	0.017	X	X	-	-	-	-
	0.050	X	X	X	X	-	-
	0.083	X	X	X	X	X	X
	0.117	-	X	X	X	X	-
	0.183	-	-	-	X	-	-

TABLE II
IRREGULAR WAVE CONDITIONS. X DENOTES A REALIZED TEST WHEREAS $-$ MEANS THAT NO EXPERIMENT WAS PERFORMED AT THESE CONDITIONS.

In irregular waves the power and the efficiency of the WEC are expressed. The instantaneous power and the mean power of the WEC are calculated according to (5) and (6), respectively.

$$P_{ins} = -F_{PTO}\dot{Z} \quad (5)$$

$$\overline{P} = \frac{\omega_m}{2\pi}\int_0^{\omega_m} -F_{PTO}\dot{Z}dt \quad (6)$$

Finally the efficiency of the WEC r is defined as the mean power of the WEC $\overline{P}$ divided by the mean power of the irregular waves $\overline{P_h}$, as defined by (7).

$$r = \frac{\overline{P}}{\overline{P_h}}, \quad \text{with} \quad \overline{P_h} = \frac{\rho g^2}{32\pi}H_{m0}^2\frac{2\pi}{\omega_m} \quad (7)$$

C. Experimental overtopping

The overtopping has been quantified according to physical tests. The water overtopping the sea wall is collected in a tank placed behind the sea wall, where two pumps with volume counters are installed. The measured overtopping quantities are directly rejected in the flume (in the calm water zone, behind the sea wall), such that the water level in the flume is not modified. The volume is collected over 300 waves for each test. Measurements of the overtopping are realised twice. The first measurements are performed in the presence of the WEC and the second without the WEC. Finally the water volume ratio overtopping the sea wall with and without the WEC $\Delta\mathcal{V}$ is expressed in (8) with $\mathcal{V}_{E_{\text{WEC}}}$ and $\mathcal{V}_E$, respectively the overtopping volume with and without the WEC.

$$\Delta\mathcal{V} = \frac{\mathcal{V}_{E_{\text{WEC}}}}{\mathcal{V}_E} \quad (8)$$

Thus if the WEC contributes to the reduction of the overtopping quantifications, we must have $\Delta\mathcal{V} < 1$

III. ANALYTICAL MODEL

The WEC is considered to be bidimensionnal (x,z plane) with a mass m defined by $m = 2\rho l\Gamma$, where ρ is the water density. The origin of the coordinate system is located at the free surface in calm water conditions. The z-axis is oriented in the upper direction and the x-axis is in the incident waves direction (Fig. 1). The only degree of freedom of the WEC is in heave motion (along z-axis). The system is virtually separated in three zones: zone 1 is located between the sea wall and the WEC, zone 2 is under the WEC, and zone 3 is the wave inlet zone (Fig. 1). Only regular waves are modelled analytically.

D. Potential flow theory

For the analytical model, potential flow theory is used. According to the fundamental principle of dynamics, the floater motion is defined using (9) where $Z(t)$ is the vertical position of the floater, g the gravity acceleration and F_S the hydrodynamic forces according to Pecher and Kofoed [28].

$$m\ddot{Z}(t) = -mg + F_S + F_{PTO} \quad (9)$$

For a potential flow, the relative pressure is expressed using the Bernoulli's equation (10), where Φ represents the velocity potential.

$$p = -\rho gZ - \rho\frac{\partial\Phi}{\partial t} - \frac{1}{2}\rho(\nabla\Phi)^2 \quad (10)$$

Considering only the first order terms to remove non-linear terms, (10) can be written following (11).

$$p = -\rho gZ - \rho\frac{\partial\Phi}{\partial t} \quad (11)$$

Integrating the pressure in (11) over the wet surface of the floater S, enable to obtain the forces acting on the WEC (12).

$$F_S = -\rho g\int_S ZdS - \rho\int_S\frac{\partial\Phi}{\partial t}dS \quad (12)$$

The first part of (12) represents the hydrostatic forces acting on the WEC and are written in (13), where $Z(t)$ is the gravity center position of the WEC.

$$\Pi = -\rho g\int_S ZdS \quad (13)$$

Considering small amplitude oscillations compared to the WEC dimensions and using the fundamental principle of dynamics, the sum of hydrostatic and gravity forces can be expressed as a spring force with the stiffness K_{Ar} (14).

$$\Pi - mg = -K_{Ar}Z \quad \text{with} \quad K_{Ar} = \frac{mg}{\Gamma} \quad (14)$$

The second part of (12) represents the hydrodynamic forces, where the potential flow Φ can be written in (15) as a sum of incident, diffracted and radiated forces according to the Haskind decomposition [29].

$$\Phi = \Phi_I + \Phi_D + \Phi_R \quad (15)$$

The incident potential is denoted by Φ_I, the diffracted potential Φ_D (corresponding to the waves reflected by a fixed WEC) and the radiated potential is denoted Φ_R (which corresponds to the waves generated by a moving WEC in still water).

Waves are supposed regular and monochromatic. The excitation force F_{ex} is computed from Φ_I and Φ_D

in (16). The effect of radiation F_r is computed from Φ_R in (17).

$$F_{ex} = -\rho \int_S \frac{\partial(\Phi_I + \Phi_D)}{\partial t} dS \quad (16)$$

$$F_R = -\rho \int_S \frac{\partial \Phi_R}{\partial t} dS \quad (17)$$

E. WEC motion equation

In linear theory, the WEC position $Z(t)$ and hydrodynamic forces are written in complex form in respectively (18) to (20), according to Folley [30] and Cruz [31]. The wave frequency is denoted ω and the complex amplitude is marked with a tilde.

$$Z(t) = \mathcal{R}_e\left[\tilde{Z}\mathrm{e}^{-i\omega t}\right] \quad (18)$$

$$F_{ex}(t) = \mathcal{R}_e\left[\tilde{F}_{ex}\mathrm{e}^{-i\omega t}\right] \quad (19)$$

$$F_R(t) = \mathcal{R}_e\left[\tilde{F}_R\mathrm{e}^{-i\omega t}\right] \quad (20)$$

Thus the complex amplitude of the radiation effect is composed of an added mass and damping term according to (21).

$$\tilde{F}_R = -\omega^2 c_m \tilde{Z} - i\omega c_a \tilde{Z} \quad (21)$$

According to (9), the WEC motion is finally written in the frequency domain as expressed in (22) and the WEC motion amplitude is expressed in (23).

$$\tilde{Z} = \frac{\tilde{F}_{ex}}{-\omega^2(m + c_m) - i\omega(c_a + B_{PTO}) + K_{Ar}} \quad (22)$$

$$a_f = |\tilde{Z}| \quad (23)$$

Following Genest [32], the optimal PTO $B_{PTO_{opt}}$ corresponds to the value of B_{PTO} when the mean absorbed power of the WEC is maximal. Thus $B_{PTO_{opt}}$ is expressed following (24).

$$B_{PTO_{opt}} = \sqrt{c_a^2 + \left(\omega(m + c_m) - \frac{K_{Ar}}{\omega}\right)^2} \quad (24)$$

To solve the motion equation in the frequency domain (22), the added mass c_m, the damping c_a and the excitation force $\tilde{F}_{ex}$ must be determined. Thus the values of the incident, diffracted and radiated potentials must be assessed, according to (16) and (17). Different identification methods have been proposed by Yang, Wu and Young [33] and by Andersen and Wuzhou [7]. Zheng, Shen and You [10] propose a method by fixing the boundaries and continuity conditions, and using the eigenfunction matching, which is developed in the following part.

F. Analytical solution

The diffracted and radiated potentials are written as a sum of N terms composed of unknown coefficients (sum of fundamental and evanescent modes) to be determined [10], [9]. The potential depends on the considered zone (1, 2 or 3) and on the floater motion (heave, roll or switch). Only the heave motion is considered. They can be written as shown in (25) and (26) for zone 1, where A'_{1n} and A_{1n} are the amplitudes of the diffracted and radiated modes.These coefficients, with those for zones 2 and 3 (A'_{2n}, B'_{2n}, A_{2n}, B_{2n} and A'_{3n}, A_{3n}) are determined by the eigenfunction matching method respectively for the diffracted and the radiated potentials. Wave numbers λ_n are defined by (27) and (28) for the propagative mode ($n = 1$) and the evanescent modes ($n > 1$), where k is the wave number and h the water depth. The reflected wave amplitude a_r is calculated from the diffracted potential in zone 3 $\Phi_D^{(3)}$ following (29) and (30).

The boundaries and continuity conditions are used in order to solve the unknown coefficients. Those conditions take into account the sea wall (total reflection of the wave). Continuity conditions of pressure and velocity are described between zones 1-2 and 2-3. Detailed description of this model can be found in Zheng, Shen and You [10].

$$\Phi_D^{(1)} = -\Phi_I(x,z) + \sum_{n=1}^{N} A'_{1n}\cosh(\lambda_n(x - D - l))\cos(\lambda_n(z + h)) \quad (25)$$

$$\Phi_R^{(1)} = -i\omega\tilde{Z}\sum_{n=1}^{N} A_{1n}\cosh(\lambda_n(x - D - l))\cos(\lambda_n(z + h)) \quad (26)$$

$$\lambda_1 = -ik, \quad \text{where } k\tanh(kh) = \frac{\omega^2}{g} \text{ for } n = 1 \quad (27)$$

$$\lambda_n \tan(\lambda_n h) = -\frac{\omega^2}{g} \quad \text{for } n > 1 \quad (28)$$

$$a_r = \left|\frac{-i\omega\Phi_D^{(3)}}{g}\right| \quad (29)$$

$$\Phi_D^{(3)} = \sum_{n=1}^{N} A'_{3n}\cos(\lambda_n(z + h))\mathrm{e}^{\lambda_n(x+l)} \quad (30)$$

To find the unknown coefficients of the diffracted and radiated potentials, each part of the equation obtained from the boundary and continuity conditions is multiplied by its eigenfunction and integrated over its respective depth interval at the floater boundaries $x = \pm l$. Thus a linear system of $4N$ equations is created according to (31) and (32) where X_D and X_R are the solution vectors of the diffracted and radiated coefficients, respectively, and S, G^D and G^R are the matrices obtained from the boundaries and continuity conditions. This linear system is solved under the PYHTON code using the GMRES algorithm with the ILU(0) preconditioner (according to Saad and Schult [34]) and the Newton algorithm is used to solve the non-linear dispersion relation.

$$SX_D = G^D \quad (31)$$

$$SX_R = G^R \quad (32)$$

The case studied by Zheng, Shen and You [10] is compared to the present code in order to be validated, i.e. $h/l = 6$, $\Gamma/h = 0.4$, $D/h = 0.2$ and $N = 30$. Dimensionless added mass, damping and excitation force are plotted in Fig. 6 and compared with results obtained by Zheng, Shen and You [10]. The presents results are identical to those of Zheng, Shen and You [10], which confirms the validity of the code.

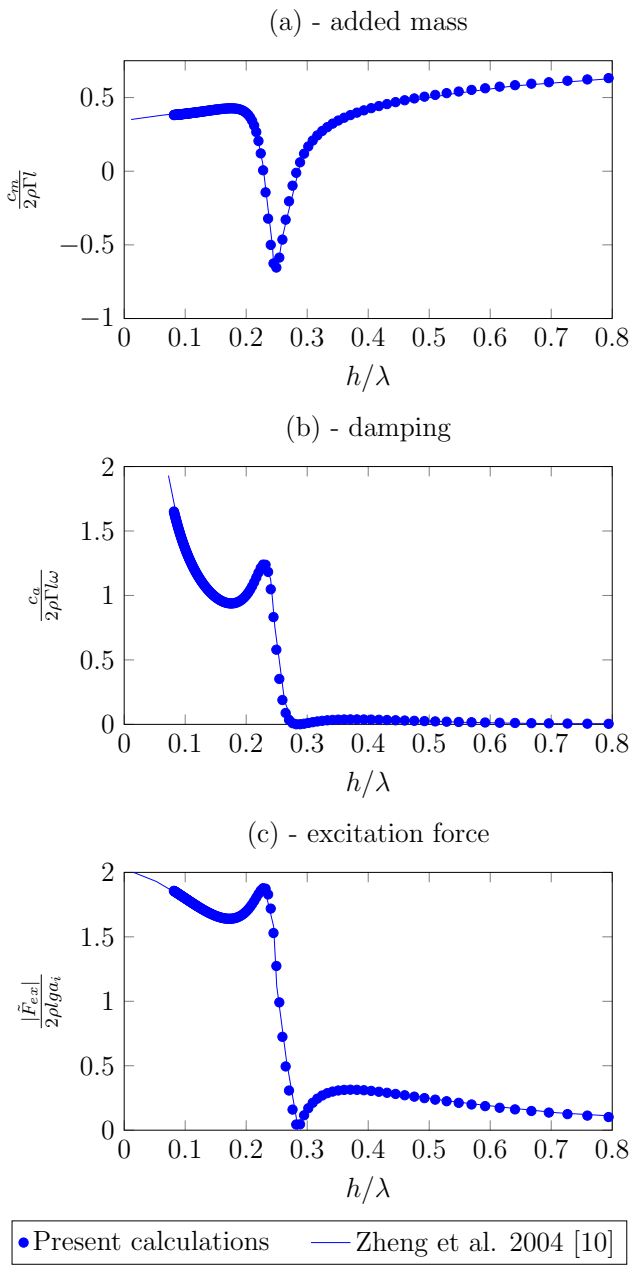

Fig. 6. (a) Variation of the dimensionless added mass. (b) damping and (c) excitation force with h/λ

The convergence of the analytical results have been quantified by varying the number of terms N in the series. The relative difference between 20 and 30 terms is 0.81% and the relative difference between 30 and 60 terms is 0.72%. For all calculations, 60 terms are used.

G. Analytical overtopping

The EurOtop guide [21] provides formulae for different types of sea walls. In this paper, the formula for a vertical wall originally suggested by Van Der Meer, Verhaeghe and Steendam [35] is used. The overtopping quantification $\mathcal{V}$ is expressed in the presence of the WEC $\mathcal{V}_{A_{\text{WEC}}}$ and without the presence of the WEC $\mathcal{V}_A$, with both quantities depending on the wave height and on the crest freeboard above the sea level R_c. Thus $\mathcal{V}_{A_{\text{WEC}}}$ is expressed with the incident analytical wave height in zone 1 $H^{(1)}/2$, removing the reflected wave height at $x = l + D$ following (33). The overtopping quantification without WEC $\mathcal{V}_A$ is expressed in (34) with the incident wave height H_i.

$$\mathcal{V}_{A_{\text{WEC}}} = 0.054 \exp\left[-\left(2.12\frac{R_c}{\frac{H^{(1)}}{2}}\right)^{1.3}\right]\sqrt{g\left(\frac{H^{(1)}}{2}\right)^3} \quad (33)$$

$$\mathcal{V}_A = 0.054 \exp\left[-\left(2.12\frac{R_c}{H_i}\right)^{1.3}\right]\sqrt{gH_i^3} \quad (34)$$

In what follows the analytical overtopping ratio $\Delta\mathcal{V}_A$ by (35).

$$\Delta\mathcal{V}_A = \frac{\mathcal{V}_{A_{\text{WEC}}}}{\mathcal{V}_A} \quad (35)$$

An improvement of the model is proposed by including the effect of the load losses between the sea wall and the WEC. According to (36), the improved analytical overtopping ratio $\Delta\mathcal{V}_A F_{corr}$ is calculated using a correction function F_{corr}. The correction function corresponds to the dimensionless difference between the fluid kinetic energy $E_c = \frac{1}{2}\rho V^2$ and the pressure losses expressed with the Darcy equation $\Delta\mathcal{P} = \frac{1}{2}\Lambda\rho V^2\frac{R_c+\Gamma}{D}$ according to Blasius [36], with V the fluid velocity and Λ the load losses coefficient.

$$F_{corr} = \frac{E_c - \Delta\mathcal{P}}{E_c} = 1 - \Lambda\frac{R_c+\Gamma}{D} \quad (36)$$

In order to determine the global optimal correction, the value of Λ is obtained by curve fitting between analytical and numerical results using the evolution strategy algorithm CMA-ES (Covariance Matrix adaptation - Evolution Strategy, Hansen [37]). Experimental and analytical tests on WEC of different dimensions without PTO are performed in order to obtained a sufficient number of overtopping values to calculate the correction. Details about the WEC and the waves conditions can be found in Neuveglise [38]. According to the CMA-ES algorithm, the global optimal value of Λ is equal to $\Lambda_{opt} = 0.012$. This value is relatively close to the values of pressure loss proposed by Savic et al. [39], Colebrook et al. [40] and Blasius [36]. Note that values proposed by these authors are obtained in steady flows, which is not the case is the present tests.

TABLE III
REGULAR WAVE CONDITIONS FOR OVERTOPPING QUANTIFICATIONS FOR WEC 1

Γ (m)	H_f (m)	l (m)	D (m)	T (s)	D/λ	R_c/D
0.25	0.40	0.05	0.005, 0.01, 0.05, 0.10, 0.25	1.16, 1.29, 1.42, 1.57, 1.67, 2.06, 2.32, 3.10, 3.35, 3.61, 3.87	8.6×10^{-5} to 0.12	14, 7, 1.4, 0.7, 0.28

TABLE IV
DIMENSIONS OF THE WECS TESTED WITH THE ANALYTICAL MODEL

Γ(m)	0.05	0.05	0.15	0.15	0.15	0.25	0.25
l(m)	0.05	0.10	0.05	0.10	0.15	0.05	0.10

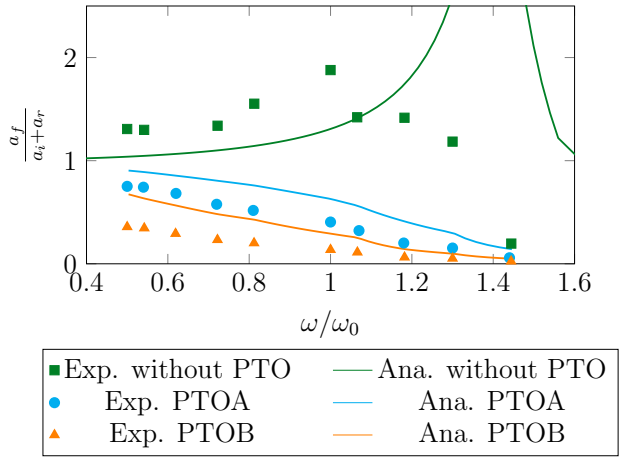

Fig. 7. Dimensionless WEC behaviour $a_f/(a_i + a_r)$ as a function of the dimensionless frequency ω/ω_0 for WEC 1 at $h = 0.6$ m in regular waves, with $\omega_0 = 3.74$ rad/s. WEC behaviour without PTO, with PTOA and with PTOB for experimental and analytical models.

To quantify the overtopping, different types of tests are performed. In a first time, the overtopping ratio with WEC 1 without PTO is estimated with the experimental and analytical models following the waves conditions presented by Table III. Thereafter different dimensions of WEC are modelled analytically and their dimensions are presented in Table IV. For those WECs, the water depth h is fixed at $h = 0.6$ m, the incident wave amplitude at $a_i = 0.25$ m, the toe clearance at $D = 0.01$ m, the value of the PTO at $B_{PTO_{opt}}$ and the wave period is varying from $T = 0.7$ s to $T = 3.87$ s.

IV. WEC BEHAVIOUR AND EFFICIENCY

H. WEC behaviour

The WEC behaviour is calculated in the presence of the PTOA, PTOB and without PTO for the analytical and experimental model. Regular waves are used. For the comparison between the two models, a reference frequency ω_0 is defined, for each tested WEC, as the frequency corresponding to the maximum motion amplitude. This frequency is determined experimentally.

First of all in Fig. 7, the WEC motion amplitude a_f of WEC 1, divided by the sum of incident and reflected wave amplitude a_i and a_r respectively, is plotted as a function of the dimensionless wave frequency ω/ω_0. The water depth h is fixed at $h = 0.6$ m. Without PTO the analytical model does not well represent the experimental WEC motion. Indeed, the maximum WEC motion amplitude obtained with the analytical model is about $a_f/(a_i+a_r) = 4.0$, when it is about twice lower with the experimental model (about $a_f/(a_i+a_r) = 1.9$). Similar results are observed concerning the resonance frequency. The analytical WEC motion resonance appears at $\omega/\omega_0 = 1.4$, when it is lower with the experimental model ($\omega/\omega_0 = 1.0$). These discrepancies may be explained by strong nonlinearities occuring for this WEC. Indeed, WEC 1 corresponds to a large draft of $\Gamma = 0.25$ m leading to strong vortices shed at the edges of the float.

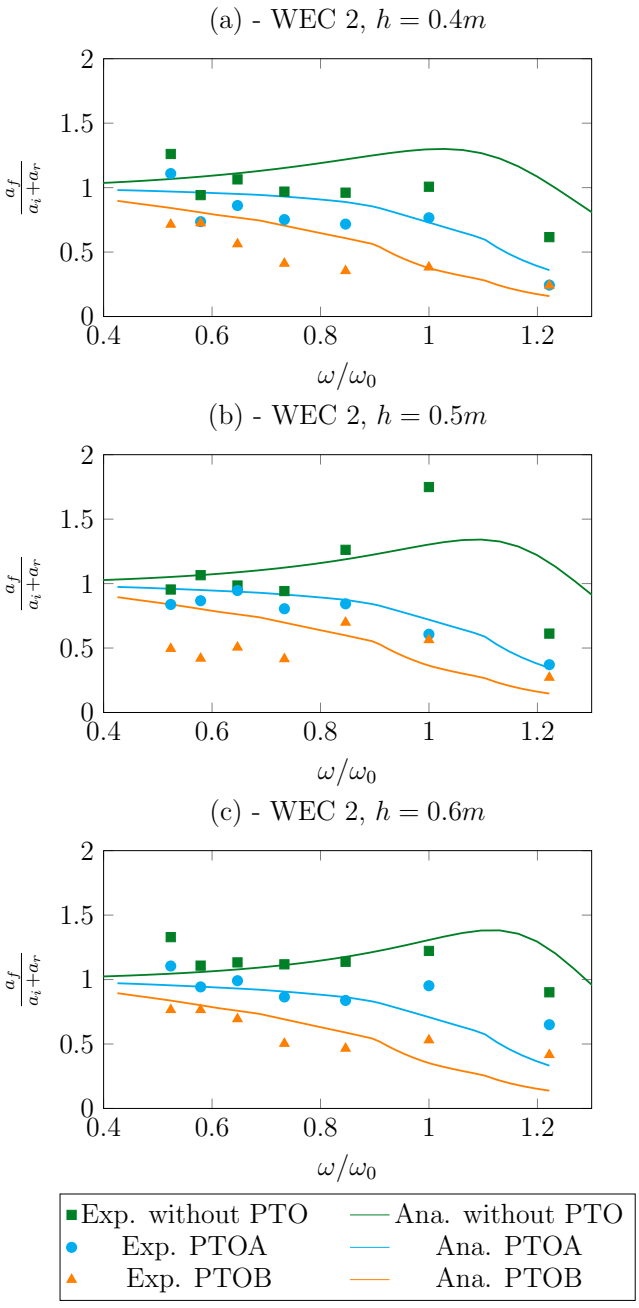

Fig. 8. Dimensionless WEC behaviour $a_f/(a_i + a_r)$ as a function of the dimensionless frequency ω/ω_0 for WEC 2 at different water depth in regular waves, with $\omega_0 = 4.43$ rad/s. WEC behaviour without PTO, with PTOA and with PTOB for experimental and analytical models. (a) - $h = 0.4$ m, (b) - $h = 0.5$ m, (c) - $h = 0.6$ m.

Secondly when PTOA or PTOB are installed, the analytical model is close to the experimental one. Indeed, values of the analytical WEC motion amplitude are slightly higher than the values obtained with the experimental model. Moreover for experimental and analytical models, the WEC motion amplitude with PTOA are higher than the WEC motion amplitude obtained with PTOB. This result was expected because the damping due to the PTO is more important with PTOB than PTOA (see Fig. 5).

In Fig. 8 the dimensionless WEC motion amplitude is presented for the WEC 2 at different water depths as a function of the dimensionless wave frequency. Analytical results are compared with experimental ones. For a

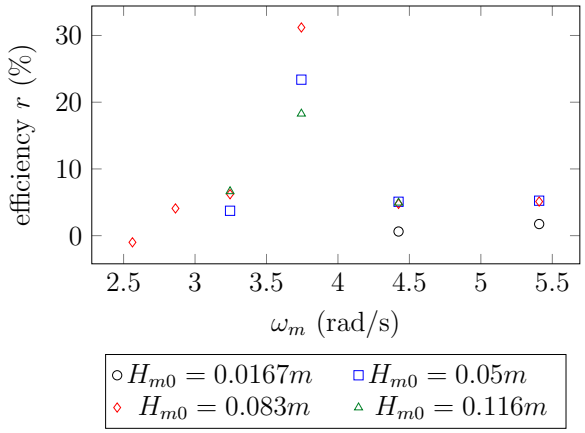

Fig. 9. Efficiency measured for WEC 2 as a function of the peak frequency in irregular waves with PTOA and at $h = 0.5$ m.

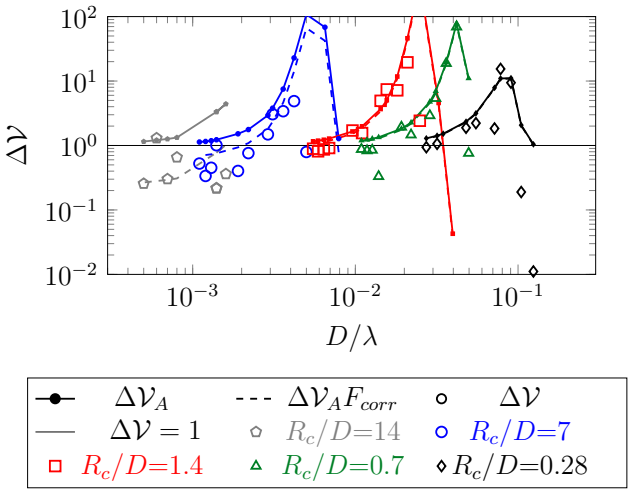

Fig. 10. Experimental ($\Delta\mathcal{V}$), initial ($\Delta\mathcal{V}_A$) and corrected ($\Delta\mathcal{V}_A F_{corr}$) analytical overtopping ratio with WEC 1 at $h = 0.6$ m, $B_{PTO} = 0$ and $a_i = 0.025$ m.

smaller draft (of $\Gamma = 0.15$ m for WEC 2), the analytical model is in good agreement with experimental results. More precisely when no PTO was added to the WEC, the analytical model is closer from experimental results when the draft is smaller (Fig. 7). At a water depth equals to $h = 0.4$ m and $h = 0.6$ m and in the presence of PTOA or PTOB, the analytical model is in good agreement with the experimental results. At $h = 0.5$ m and for low values of the dimensionless frequency ω/ω_0, the analytical model overestimates the WEC motion amplitude in the presence of PTOA or PTOB. Moreover results are globally mildly more overestimated with an higher damping (PTOB) than with a lower damping (PTOA).

I. *WEC efficiency*

Fig. 9 presents the efficiency r as a percentage depending on the peak wave frequency ω_m in irregular waves. Only experimental results have been used to calculate the efficiency. The efficiency is calculated for WEC 2 where $l = 0.15$ m, $\Gamma = 0.15$ m at a water depth $h = 0.5$ m and at $D = 0.01$ m. The higher values of the efficiency are obtained for each significant wave heights H_{m0} tested at $\omega_m = 3.7$ rad/s. This frequency value is lower than the resonance frequency of the WEC 2 in regular waves ($\omega_0 = 4.43$ rad/s, see Fig. 8). Moreover the efficiency is higher for higher values of the significant wave height at $\omega_m = 3.7$ rad/s.

According to Fig. 9 the maximum efficiency of the WEC in tested conditions is superior to 30%. The mean efficiency calculated on all tests realised in irregular wave conditions is about 7.5%. These results are rather low, however they are encouraging. It is important to remind that neither optimisation was performed on the system dimensions nor control were added to the WEC.

V. Overtopping Quantifications

In a second approach, the impact of the WEC on overtopping is presented. First of all, initial and corrected analytical overtopping ratio are compared to experimental results for WEC 1 without PTO. In Fig. 10 the overtopping ratio are plotted as a function of dimensionless number D/λ. For high values of the toe clearance (i.e. $R_c/D = 1.4,\ 0.7$ and 0.28), the initial analytical results are close to the experimental results. In addition, the corrected analytical model is very close to the initial model. At $R_c/D = 7$ and $R_c/D = 14$ and for small values of D/Λ, the values of the initial analytical model are higher than the experimental ones. In these cases, the corrected analytical model is closer to the experimental results than the initial analytical model.

Secondly, cases where $\Delta\mathcal{V} < 1$ exist. Indeed for a fixed value of R_c/D, when at the same time R_c/D is high and D/λ is small, overtopping are reduced by the presence of the WEC. The overtopping reduction also appears when D/λ is high, for a fixed value of R_c/D. According to Fig. 10, cases where the overtopping are drastically increased are also observed for intermediate values of D/λ. Thus, the dimensions of the WEC should be carefully defined in order to prevent from the increase of overtopping.

To understand the impact of the characteristics of the WEC on overtopping quantifications, different configurations of PTO have been used on WEC 1. These configurations are described in Fig. 11 where only the corrected analytical model is used. According to Fig. 11, the value of the PTO does not much influence the overtopping quantifications. Indeed, for small values of R_c/D (i.e. $R_c/D = 0.28$, 0.7 and 1.4) the values of the overtopping ratio are almost identical whatever the value of the PTO. At $R_c/D = 7$ and 14, the overtopping ratio is reduced with PTOA and PTOB compared to the curves without PTO and with the optimal PTO and for intermediate values of D/λ. For the extreme values of D/λ at $R_c/D = 7$ and 14, the overtopping ratio remains almost unchanged for different values of PTO.

Finally, overtopping ratio has been studied for different size of WEC, listed in Table IV and with the optimal PTO. According to Fig. 12, only the draft modifies the value of the overtopping ratio. Indeed for a fixed value of the draft Γ, the value of the overtopping ratio is identical for the different values of the length l. These

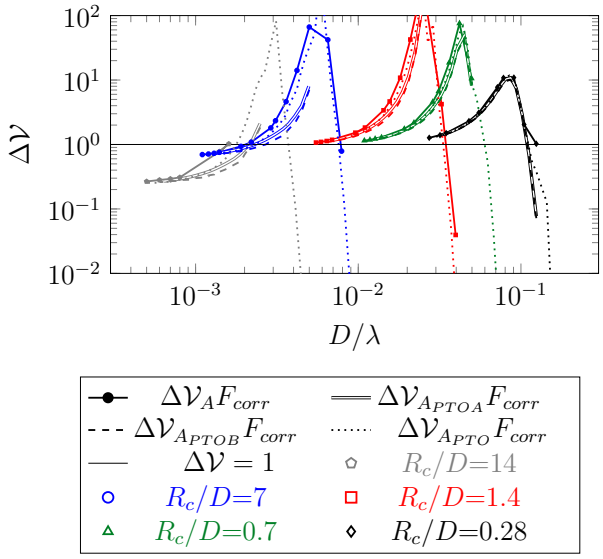

Fig. 11. Corrected analytical overtopping ratio for WEC 1 without PTO ($\Delta\mathcal{V}_A F_{corr}$), with PTOA ($\Delta\mathcal{V}_{A_{PTOA}} F_{corr}$), with PTOB ($\Delta\mathcal{V}_{A_{PTOB}} F_{corr}$) and with optimal PTO ($\Delta\mathcal{V}_{A_{PTO}} F_{corr}$) at $h = 0.6$ m and $a_i = 0.025$ m.

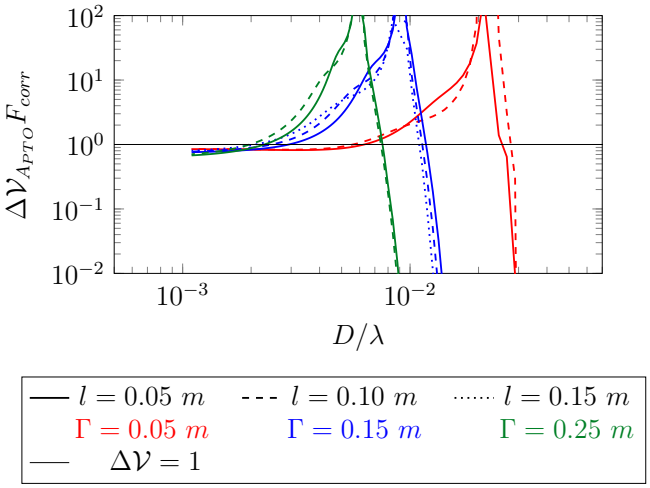

Fig. 12. Corrected analytical overtopping ratio for different WEC dimensions at $h = 0.6$ m, $a_i = 0.025$ m, $D = 0.01$ m and with the optimal PTO. The line colour represents the value of the draft Γ and the line style (solid, dashed or dashed dotted) represents the value of the half length l.

results are explained by the reduction of the WEC resonance frequency with the increased of the draft. According to Neuveglise [38] the overtopping ratio follows the WEC motion, so a decay of the resonance frequency implies a decay of the overtopping ratio.

VI. Conclusion

The behaviour of a WEC in heave motion placed in front of a sea wall has been studied. The system is composed of a rectangular floating buoy including a PTO modelled by a linear damper. The aim of this paper is twofold: study the WEC behaviour and quantify its impact on overtopping. Results obtained using an analytical model based on the potential flow theory are compared with experimental results. The analytical wave potentials and hydrodynamic coefficients are solved using the eigenfunction matching method according to Zheng et al. [10]. The overtopping are estimated analytically from the wave elevation above the sea wall using the Van Der Meer formula according to EurOtop 2016 [21]. An improvement of the analytical overtopping quantification is proposed by taking into account the load losses between the WEC and the sea wall following Neuveglise [38].

First of all, the behaviour of the WEC with different values of PTO and different wave conditions are studied in regular waves. For the WEC with the higher draft ($\Gamma = 0.25$ m) the analytical model is not reliable when no PTO was added. When the value of the PTO is increased (i.e. for PTOA and PTOB), the analytical results are close to the experimental results. For a WEC with a smaller draft at $\Gamma = 0.15$ m, the analytical model is close to experimental results for the different values of PTO tested. Thereafter the efficiency of the WEC 2 ($\Gamma = 0.15$ m and $l = 0.15$ m) has been studied in irregular waves, with wave conditions inspired from the Esquibien site. The mean efficiency obtained is about 7.5% and the maximum efficiency is superior to 30%. These results are encouraging because no optimisation was performed on the system dimensions nor on the PTO force.

In a second approach, the impact of the WEC on overtopping is quantified. In all tested cases, the analytical results appear close to the experimental model when the dimensionless number R_c/D is small (i.e. when $R_c/D \leq 1.4$). For higher values of R_c/D, the corrected analytical model is closed from experimental results than the initial analytical model. Moreover, a reduction of the overtopping quantification due to the presence of the WEC has been observed. Indeed, for small values of D and high values of λ, the overtopping are reduced by the presence of WEC 1 where the draft $\Gamma = 0.25$ m and $l = 0.05$ m. Considering these results, we were interested by the impact on the PTO value and on the size of the WEC on overtopping quantifications. From the analytical results, it has been observed that the value of the PTO does not much impact the overtopping quantifications. Similar results are observed concerning the size of the WEC : the length of the system l does not much impact the overtopping quantification in opposite to the draft Γ. Finally, the major parameters impacting the overtopping quantifications are the draft Γ, the toe clearance D and the wave length λ.

In a future work the present results should be compared with numerical simulations. Moreover it is planned to perform experimental tests measuring overtopping in a presence of PTO. Further work is necessary to improve the estimation of the WEC impact on overtopping: irregular waves will be considered to simulate more realistic wave conditions.

References

[1] A. Falcao, "Wave energy utilization: A review of the technologies," *Renewable and sustainable energy reviews*, vol. 14, no. 3, pp. 899–918, 2010.

[2] B. Drew, A. R. Plummer, and M. N. Sahinkaya, "A review of wave energy converter technology," *Proceedings of the Institution of Mechanical Engineers, Part A: Journal of Power and Energy*, vol. 223, pp. 887–902, 2009.

[3] J. Falnes, "A review of wave-energy extraction," *Marine Structures*, vol. 20, no. 4, pp. 185–201, 2007.
[4] A. Babarit and H. Mouslim, "Récupération de l'énergie des vagues," *Techniques de l'Ingenieur*, 2013.
[5] S. Astariz and G. Iglesias, "The economics of wave energy: A review," *Renewable and Sustainable Energy Reviews*, vol. 45, pp. 397–408, 2015.
[6] S. H. Salter, J. Taylor, and N. Caldwell, "Power conversion mechanisms for wave energy," *Proceedings of the Institution of Mechanical Engineers, Part M: Journal of Engineering for the Maritime Environment*, vol. 216, no. 1, pp. 1–27, 2002.
[7] P. Andersen and H. Wuzhou, "On the calculation of two-dimensional added mass and damping coefficients by simple green's function technique," *Ocean engineering*, vol. 12, no. 5, pp. 425–451, 1985.
[8] N. Drimer, Y. Agnon, and M. Stiassnie, "A simplified analytical model for a floating breakwater in water of finite depth," *Applied Ocean Research*, vol. 14, no. 1, pp. 33–41, 1992.
[9] Y. Zheng, Y. You, and Y. Shen, "On the radiation and diffraction of water waves by a rectangular buoy," *Ocean Engineering*, vol. 31, no. 8-9, pp. 1063–1082, 2004.
[10] Y. Zheng, Y. Shen, Y. You, B. Wu, and D. Jie, "On the radiation and diffraction of water waves by a rectangular structure with a sidewall," *Ocean Engineering*, vol. 31, no. 17-18, pp. 2087–2104, 2004.
[11] S. Zheng and Y. Zhang, "Wave diffraction from a truncated cylinder in front of a vertical wall." *Ocean Engineering*, vol. 104, pp. 329–343, 2015.
[12] ——, "Wave radiation from a truncated cylinder in front of a vertical wall." *Ocean Engineering*, vol. 111, pp. 602–614, 2016.
[13] S. Mavrakos, G. Katsaounis, K. Nielsen, and G. Lemonis, "Numerical performance investigation of an array of heaving wave power converters in front of a vertical breakwater." in *14th Int. Offshore and Polar Engineering Conf., Toulon, France*, 2004.
[14] M. Penalba, T. Kelly, and J. V. Ringwood, "Using nemoh for modelling wave energy converters: A comparative study with wamit," in *Proceedings of the 12th European Wave and Tidal Energy Conference (EWTEC2017), Cork, Ireland*, 2017.
[15] A. Babarit and G. Delhommeau, "Theoretical and numerical aspects of the open source bem solver nemoh," in *11th European Wave and Tidal Energy Conference (EWTEC2015), Nantes, France*, 2015.
[16] A. Roessling and J. Ringwood, "Finite order approximations to radiation forces for wave energy applications," in *Renewable energies offshore*, C. G. Soares, Ed. CRC Press, 2015, pp. 359–366.
[17] B. Zanuttigh and E. Angelelli, "Experimental investigation of floating wave energy converters for coastal protection purpose," *Coastal Engineering*, vol. 80, pp. 148–159, 2013.
[18] V. Stratigaki, "Modelling of wave attenuation induced by multi-purpose floating structures used for power supply and coastal protection," in *PIANC Yearbook 2015*. PIANC, 2014, pp. 135–146.
[19] E. Mendoza, R. Silva, B. Zanuttigh, E. Angelelli, T. L. Andersen, L. Martinelli, J. Q. H. Nørgaard, and P. Ruol, "Beach response to wave energy converter farms acting as coastal defence," *Coastal Engineering*, vol. 87, pp. 97–111, 2014.
[20] J. De Waal and J. Van Der Meer, "Wave runup and overtopping on coastal structures," in *Coastal Engineering Proceedings*, 1992, pp. 1758–1771.
[21] J. Van der Meer, N. Allsop, T. Bruce, J. De Rouck, A. Kortenhaus, T. Pullen, H. Schüttrumpf, P. Troch, and B. Zanuttigh, *EurOtop 2016. Manual on wave overtopping of sea defences and related structures. An overtopping manual largely based on European research, but for worldwide application. www.overtopping-manual.com*, 2016.
[22] S. Shao, C. Ji, D. I. Graham, D. E. Reeve, P. W. James, and A. J. Chadwick, "Simulation of wave overtopping by an incompressible sph model," *Coastal Engineering*, vol. 53, no. 9, pp. 723–735, 2006.
[23] Y. Goda, *Random seas and design of maritime structures*. World Scientific Publishing Company, 2010.
[24] E. P. Mansard and E. R. Funke, "The measurement of incident and reflected spectra using a least squares method," in *Coastal Engineering Proceedings*, 1980, vol. 17, pp. 154–172.
[25] Y. Goda and Y. Suzuki, "Estimation of incident and reflected waves in random wave experiments," in *Coastal Engineering Proceedings*, 1976, vol. 15, pp. 828–845.
[26] K. Hasselmann, T. Barnett, E. Bouws, H. Carlson, D. Cartwright, K. Enke, J. Ewing, H. Gienapp, D. Hasselmann, P. Kruseman *et al.*, "Measurements of wind-wave growth and swell decay during the joint north sea wave project (jonswap)," *Ergänzungsheft 8-12*, 1973.
[27] B. Michard, E. Cosquer, A. Mallegol, J. Coignard, J. Filipot, K. Kpogo Nuwoklo, M. Olagnon, and P. Sergent, "Projet emacop: caractérisation des vagues et du potentiel houlomoteur des sites desquibien et de saint-guénolé par simulation numérique," in *XIVèmes Journées Nationales Génie Côtier–Génie Civil, 29 juin-1er juillet 2016, Toulon*, 2016.
[28] A. Pecher and J. P. Kofoed, *Handbook of Ocean Wave Energy*. Springer, 2017.
[29] M. Haskind and J. Newman, "The exciting forces and wetting of ships in waves," David Taylor Model Basin Washington DC, Tech. Rep., 1962.
[30] M. Folley, *Numerical Modelling of Wave Energy Converters: State-of-the-Art Techniques for Single Devices and Arrays*. Academic Press, 2016.
[31] J. Cruz, *Ocean wave energy: current status and future prespectives*. Springer Science & Business Media, 2007.
[32] R. Genest, "Dveloppement et validation exprimentale de stratgies de contrle des rcuprateurs de l'nergie des vagues," Ph.D. dissertation, Ecole Centrales de Nantes, 2014.
[33] F.-L. Yang, C. T. Wu, and D. L. Young, "On the calculation of two-dimensional added mass coefficients by the taylor theorem and the method of fundamental solutions," *Journal of Mechanics*, vol. 28, no. 1, pp. 107–112, 2012.
[34] Y. Saad and M. H. Schult, "Gmres: A generalized minimal residual algorithm for solving nonsymmetric linear systems," *SIAM Journal on scientific and statistical computing*, vol. 7, no. 3, pp. 856–869, 1986.
[35] J. W. Van Der Meer, H. Verhaeghe, and G. J. Steendam, "The new wave overtopping database for coastal structures," *Coastal Engineering*, vol. 56, no. 2, pp. 108–120, 2009.
[36] H. Blasius, "Stromfunktion fur die stromung durch turbinenschaufeln," *Z Math Phys 59*, pp. 225–243, 1911.
[37] N. Hansen, "The cma evolution strategy: a comparing review," in *Towards a new evolutionary computation: Advances in estimation of distribution algorithm*. Springer, 2006, pp. 75–102.
[38] S. Neuveglise, "Modlisation numrique et physique de la chane de rcupration de l'nergie de la houle par un dispositif bord quai," Ph.D. dissertation, Université Le Havre Normandie, France, 2018.
[39] V. Savić, D. Knežević, D. Lovrec, M. Jocanović, and V. Karanović, "Determination of pressure losses in hydraulic pipeline systems by considering temperature and pressure," *Strojniški vestnik-Journal of Mechanical Engineering*, vol. 55, no. 4, pp. 237–243, 2009.
[40] C. F. Colebrook, T. Blench, H. Chatley, E. Essex, J. Finniecome, G. Lacey, J. Williamson, and G. Macdonald, "Correspondence. turbulent flow in pipes, with particular reference to the transition region between the smooth and rough pipe laws. (includes plates)." *Journal of the Institution of Civil engineers*, vol. 12, no. 8, pp. 393–422, 1939.